Science Advances

AAAS

advances.sciencemag.org/cgi/content/full/3/6/e1603210/DC1

Supplementary Materials for

Electronic structure of aqueous solutions: Bridging the gap between theory and experiments

Tuan Anh Pham, Marco Govoni, Robert Seidel, Stephen E. Bradforth, Eric Schwegler, Giulia Galli

Published 23 June 2017, *Sci. Adv.* **3**, e1603210 (2017)
DOI: 10.1126/sciadv.1603210

This PDF file includes:

Photoelectron spectra of the $NaNO_3$ solution

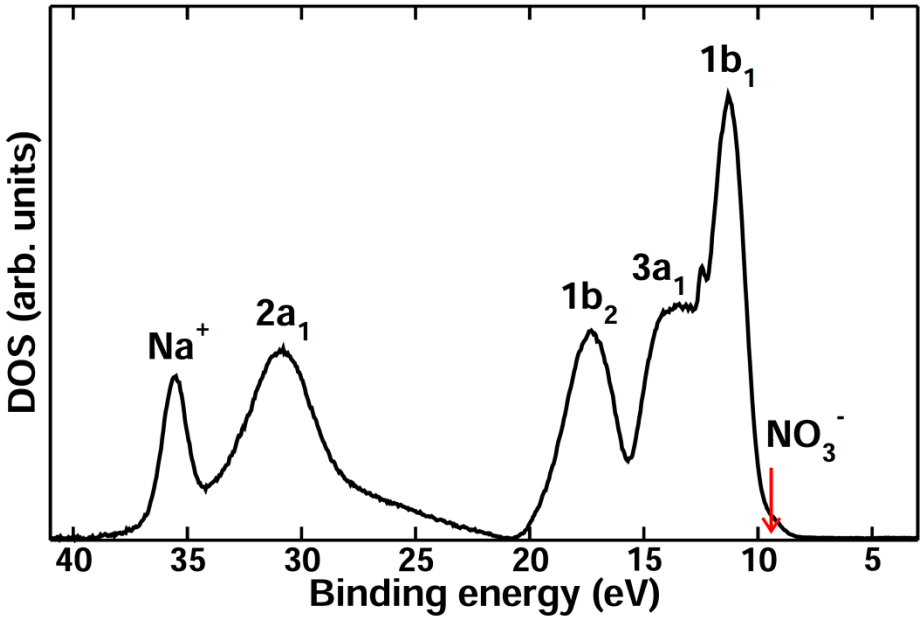

fig. S1. Photoelectron spectra of a 1.0 M $NaNO_3$ solution measured by the liquid-jet technique. Emission from the water valence orbitals ($1b_1$, $3a_1$, $1b_2$ and $2a_1$) and from aqueous ions (Na^+ and NO_3^-) is labeled. The peak at 35.4 eV corresponds to electrons ejected from Na^+ ions.

Calculated CO_3^{2-} IPs for different simulation trajectories

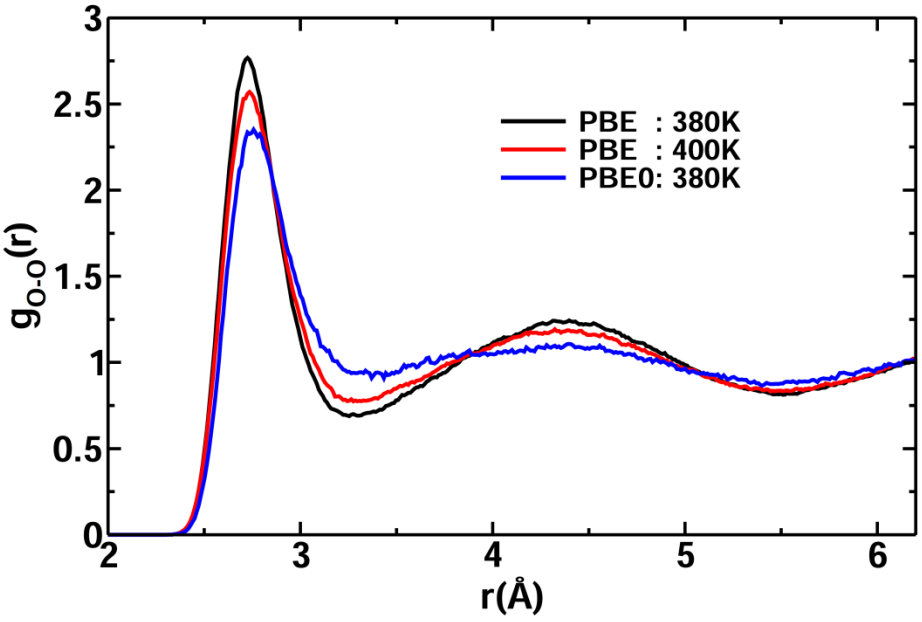

fig. S2. Radial distribution functions of water molecules computed for CO_3^{2-} solutions generated using PBE at 380 K (black) and 400 K (red) and using PBE0 at 380 K (blue).

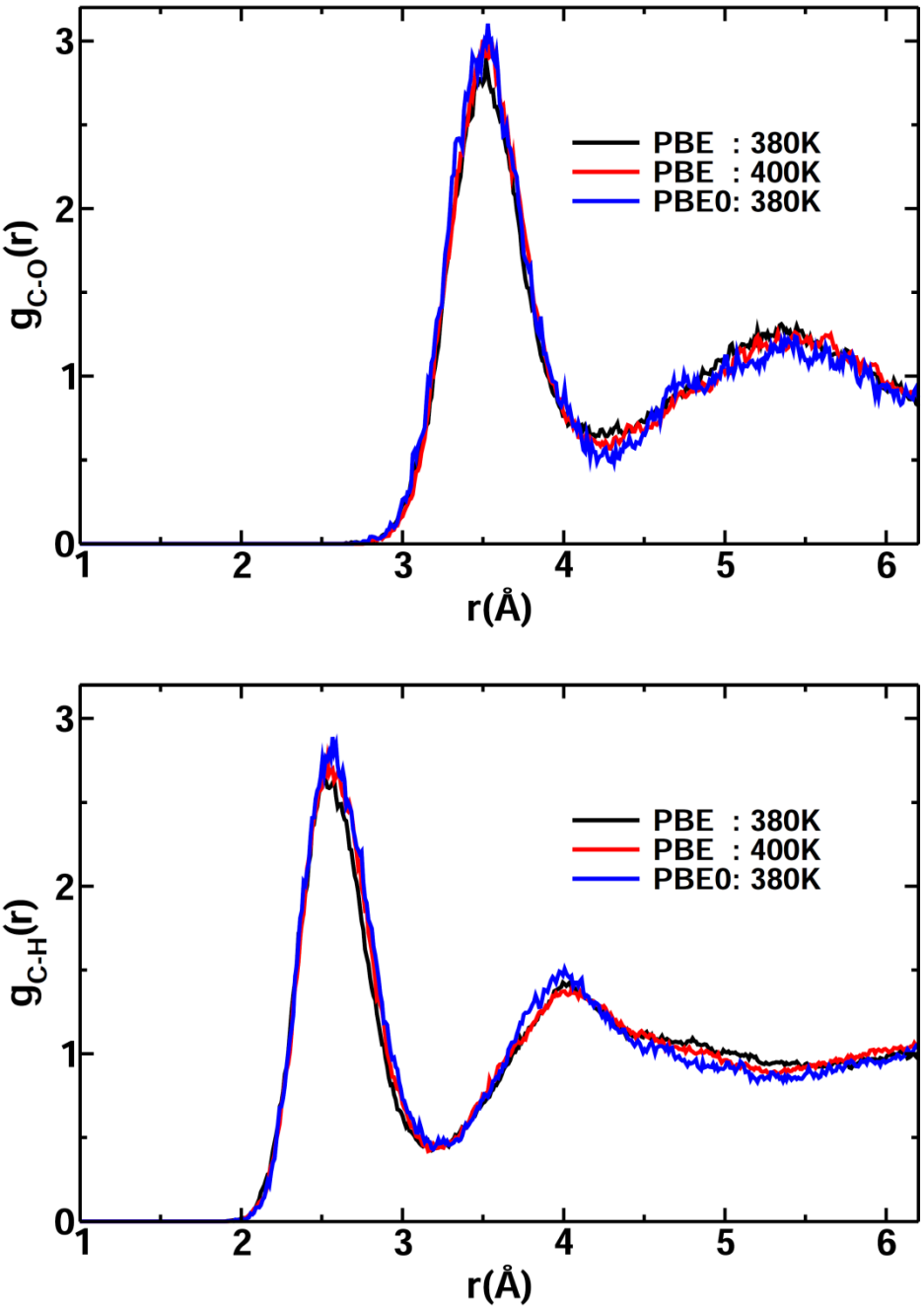

fig. S3. Radial distribution functions of carbon-water oxygen and carbon-water hydrogen computed for CO_3^{2-} solutions generated using PBE at 380 K (black) and 400 K (red) and using PBE0 at 380 K (blue).

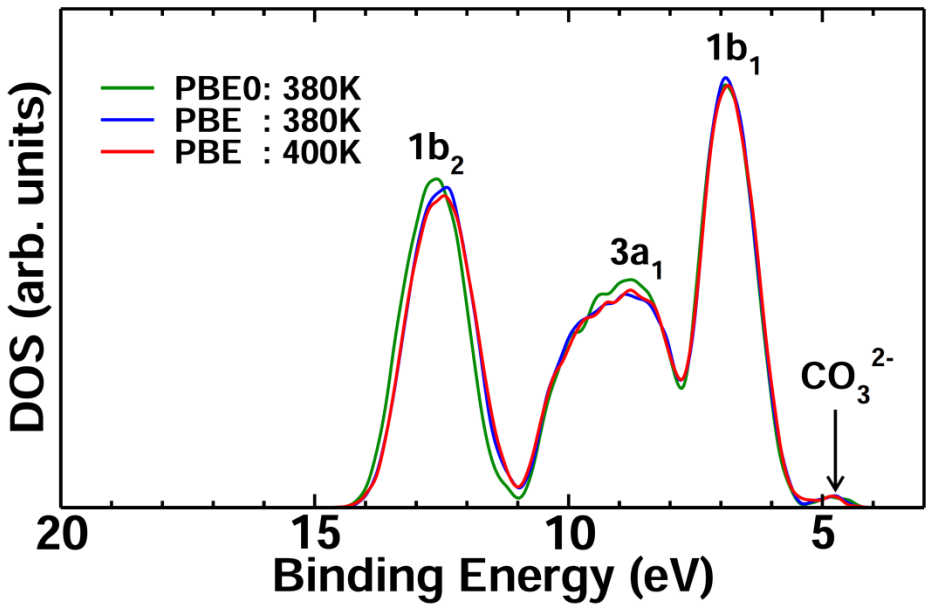

fig. S4. DOS computed with DFT and the PBE functional for CO_3^{2-} solutions generated with PBE at 400 K (red), PBE at 380 K (blue), and PBE0 at 380 K (green). All energy levels are relative to vacuum.

IPs of solvated ions

table S1. IPs (eV) of selected solvated ions computed using DFT with RSH and sc-hybrid density functionals, compared with PE liquid-jet measurements. Theoretical standard deviations were obtained by averaging results over 100 configurations extracted from molecular dynamics simulations. The variation in the experimental results represents the range of different IP due to ion concentration, counterion and ionic strength effects.

Ion	Experiment	RSH	sc-hybrid
$SeCN^-$	7.84±0.09	7.29±0.27	7.43±0.27
SO_3^{2-}	7.84±0.08	7.58±0.27	7.84±0.28
SCN^-	8.17±0.08	7.70±0.27	7.94±0.28
ClO_2^-	8.22±0.09	8.04±0.34	8.42±0.35
CO_3^{2-}	8.30±0.16	8.37±0.27	8.80±0.27
PO_4^{3-}	8.54±0.08	8.32±0.24	8.73±0.25
NO_2^-	8.58±0.16	8.54±0.40	8.98±0.41
ClO^-	8.59±0.10	8.38±0.38	8.75±0.39

HPO_4^{2-}	9.05±0.12	8.74±0.31	9.16±0.32
OCN^-	9.15±0.10	8.80±0.45	9.13±0.35
SO_4^{2-}	9.19±0.09	8.94±0.26	9.40±0.27
NO_3^-	9.42±0.18	9.21±0.33	9.70±0.33
CN^-	9.60±0.11	9.60±0.26	9.83±0.22
ClO_3^-	9.66±0.11	9.20±0.31	9.63±0.29
HCO_3^-	9.77±0.10	9.27±0.28	9.72±0.25
ClO_4^-	10.07±0.11	9.72±0.26	10.26±0.27

Finite-size effects

In R. Ayala *et al.*, the finite-size correction to the energy of an aqueous model system was derived using the Born cavity model: $\Delta E = q^2\xi/2\varepsilon V^{1/3} - (1-1/\varepsilon)2q^2R^2/3V$, where q and R are the charge and cavity radius of the ion, respectively; ξ is the Madelung constant, V is the volume of the supercell, and ε is the dielectric constant of the solution model. When the static dielectric constant of liquid water is used $\varepsilon_0=78$, the leading contribution that is proportional to $\varepsilon^{-1}V^{-1/3}$ is small, e.g., on the order of 0.1 eV for the NO_3^- ion for the supercell employed in this work. The second order correction may then play an important role. For example, calculations using point charge models for solvated iron ions showed that the contribution of the second order correction to the vertical transition energy could be as large as more than 1.0 eV for the system size considered here (*52*). However, this contribution is likely an exaggeration as it was obtained using classical point charge models, where delocalization effects are not included, in contrast to direct FPMD simulations (*47*).